

# RING RESONATORS IN POLYMER FOILS FOR SENSING OF GASEOUS SPECIES

Elke Pichler<sup>a</sup>, Konrad Bethmann<sup>b</sup>, Urs Zywiets<sup>c</sup>, Christian Spad<sup>a</sup>, Uwe Gleissner<sup>d</sup>, Christian Kelb<sup>e</sup>, Bernhard Roth<sup>e</sup>, Carsten Reinhardt<sup>c</sup>, Ulrike Willer<sup>a</sup>, Wolfgang Schade<sup>a,b\*</sup>

<sup>a</sup> Clausthal University of Technology, Institute for Energy Research and Physical Technologies (IEPT) and Energy Research Center of Lower Saxony (EFZN), Am Stollen 19B, 38640 Goslar, Germany,

<sup>b</sup> Fraunhofer Heinrich Hertz Institute, Fiber Optical Sensor Systems, Am Stollen 19B, 38640 Goslar, Germany  
<sup>c</sup> Laser Zentrum Hannover e.V. (LZH), Hollerithallee 8, 30419 Hannover, Germany

<sup>d</sup> Department of Microsystems Engineering (IMTEK), University of Freiburg, Georges-Köhler-Allee 106, 79110 Freiburg, Germany

<sup>e</sup> Hannover Centre for Optical Technologies (HOT), Nienburger Straße 17, 30167 Hannover, Germany

## ABSTRACT

In this paper, the concept of a micro ring resonator formed of waveguides in off-the-shelf polymers is presented. Extensive simulations were performed to determine appropriate dimensions for the waveguide and the design of ring and coupling zone as well as for the estimation of losses. Based on the calculated parameters, a first polymer ring resonator was realized using microscope projection lithography.

Keywords: Detection of gases, ring resonator, evanescent field, polymer waveguide

## 1. INTRODUCTION

Direct sensing of gaseous species is of great importance for a variety of applications, as e.g. environmental monitoring, process control and controlling of standards for workspace safety. Optical methods have gained much interest because they need no sample preparation and enable in situ and online detection of low concentrations. However, for conventional detection methods, a free optical path is needed, which is not practical for some applications. Here, optical evanescent field sensors have become important devices. They rely on the interaction of light guided within an optical waveguide with gases or liquids surrounding the waveguide. This interaction is possible, because the electromagnetic field penetrates from the waveguide into the surrounding optical thinner medium; since its amplitude decreases exponentially, it is called evanescent field.

Micro ring resonators rely on changes of refractive indices by adsorption of molecules on the surface of waveguides. Manufactured with well established silicon-nitride wafer technology and functionalized by coating with receptor molecules, they are already being used successfully for sensitive and selective detection; e.g. with receptors based on triphenylene-ketal, detection of the explosive TNT could be demonstrated down to concentrations of 300 ppt<sup>1</sup>.

The transfer of this sensing principle to cost efficient and easy to process materials like polymers would open new fields of application since sensor networks could be easily realized within a foil.

In this paper, the concept of a micro ring resonator formed of waveguides in polymers is presented.

## 2. METHODOLOGY

### Sensing principle

The basic setup of a micro ring resonator is shown in Fig.1. It consists of a straight waveguide that transverses in the coupling zone in close vicinity to a closed waveguide, here depicted as ring. However, also different geometrical forms like race-tracks are used. Light guided within the straight waveguide can couple to the closed one and vice versa via evanescent coupling since they are separated by only a few micrometers. After traversing the ring, the phase shifted light

which couples back into the straight waveguide interferes destructively with the light that did not enter the ring. When the frequency of the input light is tuned over the resonance frequency of the micro ring this effect leads to a dip within the transmitted intensity. It occurs when the resonance condition given in equation (1) is fulfilled.

$$m \lambda = n_{\text{eff}} L_R \tag{1}$$

Here,  $m$  is the resonance order,  $\lambda$  the wavelength,  $L_R$  the perimeter of the ring and  $n_{\text{eff}}$  describes the effective refractive index of the waveguides. This equation shows a strong dependence of the resonance frequency on the effective refractive index, thus a small change in  $n_{\text{eff}}$ , e.g. caused by the adsorption of analytes on the surface of the micro ring, leads to a shift of the resonance dip.

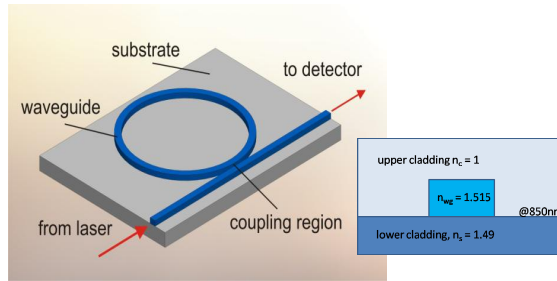


Figure 1. Schematic of a ring resonator and the ridge waveguide (small insert).

The detection limit for micro ring resonators is proportional to  $(QS)^{-1}$ , where  $Q$  is the quality factor, and  $S$  the sensitivity, which depends mainly on the penetration depth of the evanescent field into the surrounding and the change of the refractive index caused by adsorption of the analytes. Ridge waveguides as depicted in figure 1 are used in order to maximize the surface area of the waveguides that is in contact with the surrounding gas.

The sensor device was built on low cost off-the-shelf material: PMMA is used as substrate and ormosil, a photosensitive, zirconium sol gel material<sup>[2]</sup> as the core material.

### 3. SIMULATION AND DESIGN OF A SENSOR BASED ON A MICRO RING RESONATOR

Simulations have been carried out in order to determine the waveguide’s geometrical dimensions and the needed gap between the waveguides as well as to estimate the contribution of different loss mechanisms. For the investigation of the losses due to the surface the simulation tool BeamPROP™ of the RSOFT CAD Environment™ has been used, all other simulations have been carried out with the fully vectorial mode solver tool FIMMWAVE Photon Design®. The main contributions are diffraction losses due to bending of the waveguide and losses due to the roughness of the waveguide walls.

#### Simulations on single mode behavior

Single mode waveguides are essential for the clear detection of interference effects. Therefore it is important to find the ideal geometry for the waveguides that are producible in polymers and allow for single mode wave guiding. The refractive indices of the used off-the-shelf materials that were used in the simulations are given in Table 1.

Table 1: Refractive indices of the used materials.

Substrate	PMMA	$n_s$	1.49 @ 850nm
Waveguide	ormosil	$n_w$	1.55 @ 850nm
Upper cladding	air	$n_c$	1.00 @ 850nm

As the surrounding medium of the sensor device will gaseous, the refractive index of air was used for the upper cladding as a first approximation. Simulations were carried out for a wavelength of  $\lambda=850\text{nm}$ .

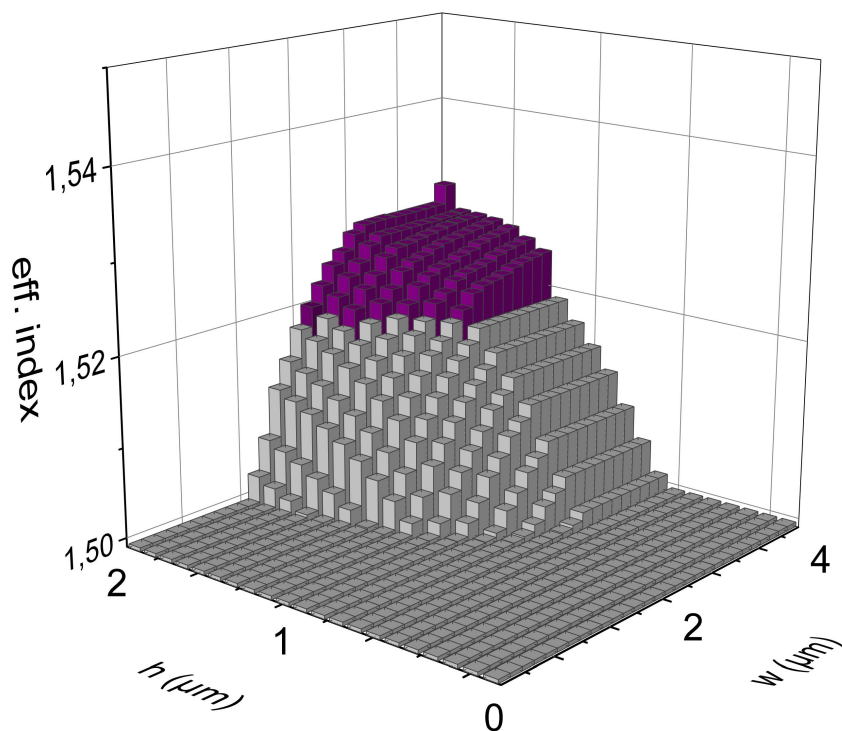


Figure 2: Results of the simulation for the waveguide calculated with FIMMWAVE Photon Design® With the refractive indices of the substrate  $n_s = 1.49$ , the refractive index of the upper cladding  $n_c = 1$  and  $n_w = 1.55$  for the waveguide .

A waveguide structure is called single mode if just the two fundamental modes, the TM and the TE mode, are guided. The results of the simulation for the given waveguide materials is shown in Fig 2. As no light can be guided when the effective refractive index of the mode is lower than  $n_s$  of the substrate, all solution smaller than this where set to zero. The light gray bars represent the single mode region of the waveguide and the dark bars represent the transition to the multimode region.

### Coupling efficiency

An important parameter for a micro ring resonator is the coupling factor  $T = |E_{out}/E_{in}|^2$ , which describes the efficiency for coupling between the ring and the straight waveguide, with  $|E_{out}|^2$  the transmitted power, and  $|E_{in}|^2$  the power of the incoupled light. From previous work with silicon-nitride waveguides on silicon, a coupling coefficient of about 5 % has been proven to be useful for gas detection<sup>7</sup>

Simulations with various gap dimensions were performed to identify the separation for the waveguides for a coupling factor close to 5%. The results are shown in Fig 3. Since all loss mechanisms have been neglected for these simulations, the coupling factor is expected to be smaller for the actual device with these dimensions.

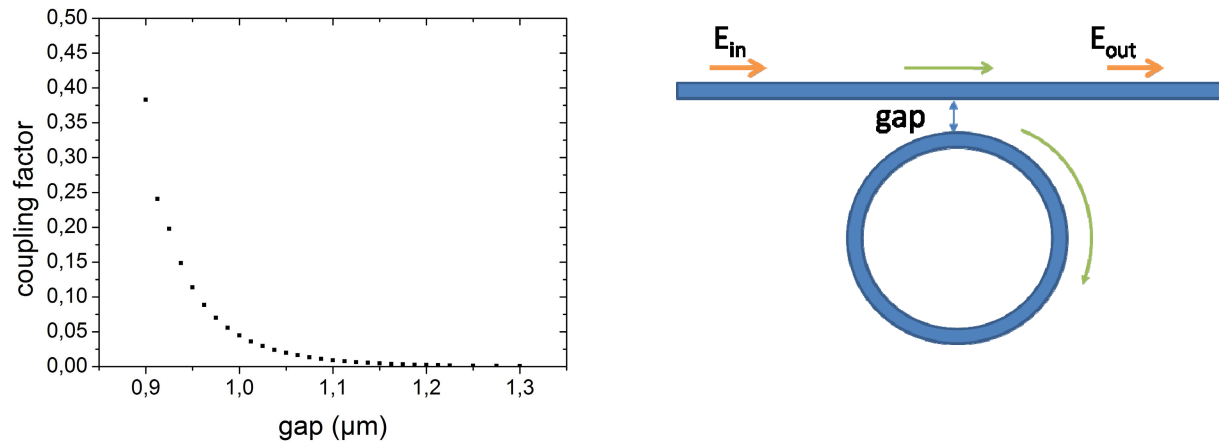


Figure 3 (a) Simulation of the coupling factor for different gaps between the ring resonator and the straight waveguide (left) and a schematic drawing of the ring resonator sensor (right).

### Loss simulations

Optical losses in a polymer waveguide result from different mechanisms: extrinsic and intrinsic scattering and absorption. As both used materials, PMMA and ormosil, are highly transparent at the used wavelength of  $\lambda=850\text{nm}$ , absorption can be neglected. By carefully processing of the polymer intrinsic scattering due to density fluctuations in the material, stress induced scattering losses and also extrinsic scattering losses caused by surface contaminations and remaining monomers can be minimized and also neglected. The main losses in the discussed micro ring resonator occur because of losses due to the radius of curvature of the ring and because of surface roughness.

### Losses in bent waveguides

For the dimension of the waveguide a set of values received from previous simulations was used. As can be seen in Fig 4 the bend losses depend strongly on the difference  $\Delta n$  between the refractive indices  $n_s$  of the substrate and  $n_w$  of the waveguide material. Smaller contrast  $\Delta n$  allows smaller bend radii. Bigger waveguide dimensions also have lower bend losses.

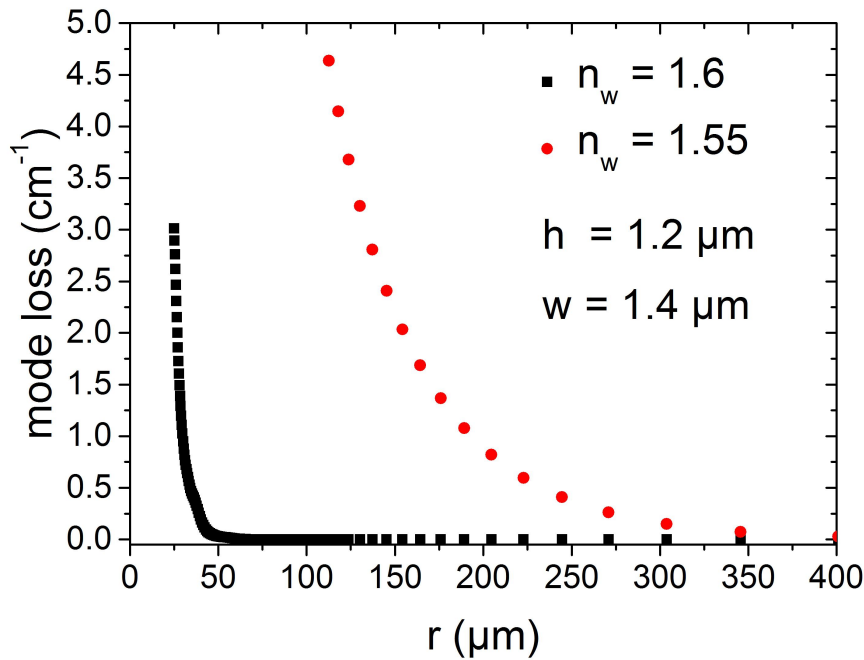


Figure 4: Simulation results: Bend losses of a circularly curved ridge waveguide with height  $h = 1.2 \mu\text{m}$  and width  $w = 1.4 \mu\text{m}$ .

### Surface roughness

The losses caused by surface roughness are inversely proportional the wavelength and proportional to the root mean square surface roughness  $\sigma$ , the square of the index contrast  $\Delta n$  of the core and cladding materials and the intensity of the light field at the surface of the waveguide. As a considerable part of the TE and the TM modes in a single mode waveguide is guided close to the surface, the losses are dominated by the surface roughness<sup>3</sup>.

The simulation tool BeamPROP™ considers the same roughness for all waveguide walls. Therefore, the simulated losses overestimate the losses since the fabrication technique results in smaller surface roughness of the upper wall than the side walls (refer to Fig. 5), which means that the real waveguides have considerably lower losses. However, the simulations provide a useful upper limit for the scattering losses and with these results a cost efficient production technique can be found. In Fig 5 the results for a waveguide with the width  $w$  and high  $h = 1.5\mu\text{m}$  is shown.

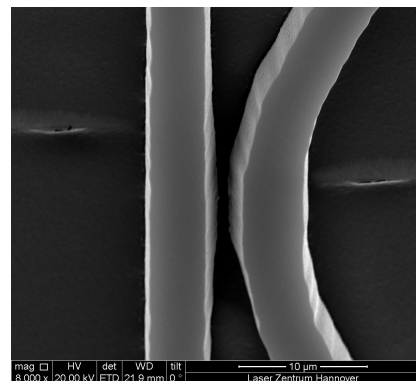
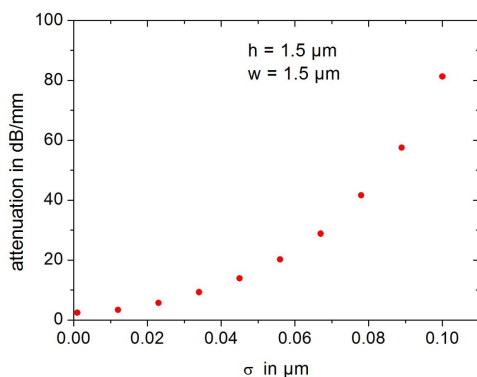


Fig. 5: Simulation results for a ridge waveguide with height  $h = 1.5\mu\text{m}$  and width  $w = 1.5\mu\text{m}$ . REM-image of the gap between the straight waveguide and the resonator ring of the first produced ring. The surfaces have an estimated surface roughness of far below  $0.2\mu\text{m}$ .

## Design parameters

The design of the ring resonator is driven by different constraints regarding material parameters and losses induced by geometry or production technique. For the used materials, the possible combinations of waveguide width  $w$  and height  $h$  can be extracted from Fig. 2 for achieving guidance of the fundamental modes only, which is essential for a clear interference signal. A radius of curvature below  $50\ \mu\text{m}$  should be avoided due to rapidly increasing bend losses. A band gap of about  $1\ \mu\text{m}$  provides a coupling between the waveguide and the ring of about 5 %, which promises good results for the gas measurement. The surface roughness should be small, values lower than  $\sigma = 0.2\ \mu\text{m}$  are acceptable. More details of the simulations can be found in<sup>[4]</sup>.

In Figure 6 the simulation for the transmitted intensity for an ideal micro ring resonator are shown. The gap between the ring and the straight waveguide is chosen to be  $g = 1\ \mu\text{m}$ . This spacing was used because of the good results for a coupling factor of about 5%. The radius of the ring is  $50\ \mu\text{m}$ . Based on the simulation results and adapted to the constraints of the fabrication technique, a first micro ring resonator was fabricated. The waveguide has the height  $h = 3.3\ \mu\text{m}$ , and width  $w = 5.2\ \mu\text{m}$ . The radius of the ring is  $50\ \mu\text{m}$ .

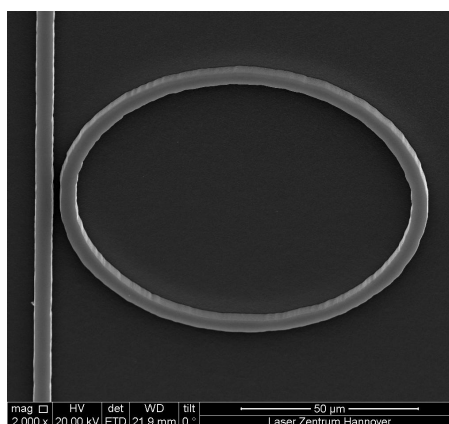
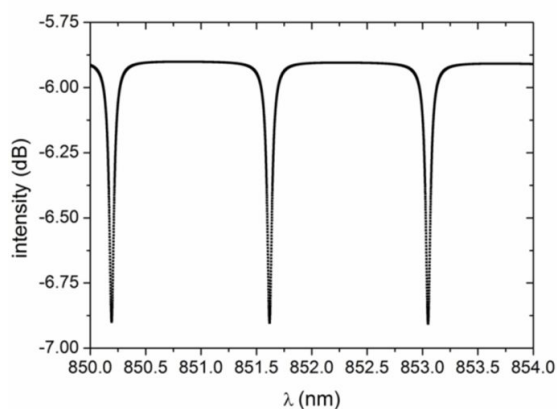


Figure 6: Simulation of transmitted signal for the ideal simulated waveguide and REM image of the first processed ring resonator.

## 4. EXPERIMENTAL RESULTS

### First micro ring resonator

Based on the simulation results first polymer micro ring resonators (refer to Figure 7) were fabricated in a photosensitive, zirconium sol gel material by microscopic projection photolithography (MPP). General information about this method can be found in<sup>5</sup>. The geometrical size of the processed waveguides differs slightly from the provided design parameters. However, with further maturation of the technique and including the constraints into the design, a better resemblance is expected for the next batches.

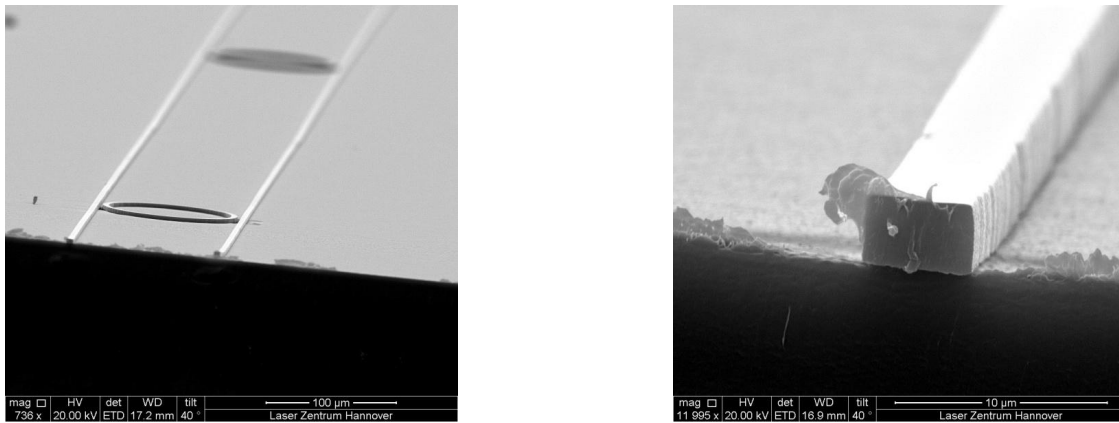


Figure 7. Micro ring resonator, ormosil on PMMA foil. The waveguides have a width  $w$  of  $5.2\mu\text{m}$  and a high  $h$  of  $3.3\mu\text{m}$ . The radius of the ring is  $100\mu\text{m}$  and the gap between the straight waveguide and the ring is  $1\mu\text{m}$

### Preparation of the end facets

To couple light into the waveguide, the end facets of the input and output channels have to be prepared. For this, a self-made POF-cleaver was used (refer to Figure 8, designed according to results of Stefani et al.<sup>[6]</sup> and Abdi et al.<sup>7</sup> who aimed at cleaving techniques for photonic-crystal-POF. The cleaver consists of a heated base plate and a heated razorblade on linear guides, both independently temperature-controlled by a two-level controller. The cleaving at higher temperature allows a ductile cutting of the samples, avoiding a brittle fracturing that would lead to undesirable surface quality.

During the cleaving process, the sample is first placed on the plate and given some time to reach thermal equilibrium, depending on the sample thickness. After that, the blade is manually lowered onto the sample and by manual application of force the sample is cut. Typically, cleaving results show a homogenous cut for most of the cutting length, followed by a brittle fracture when the remaining cross section is forced apart by the v-form of the blade. For our samples, with embedded or surface-located waveguides, the waveguides were always cut ductile, showing satisfactory surface quality

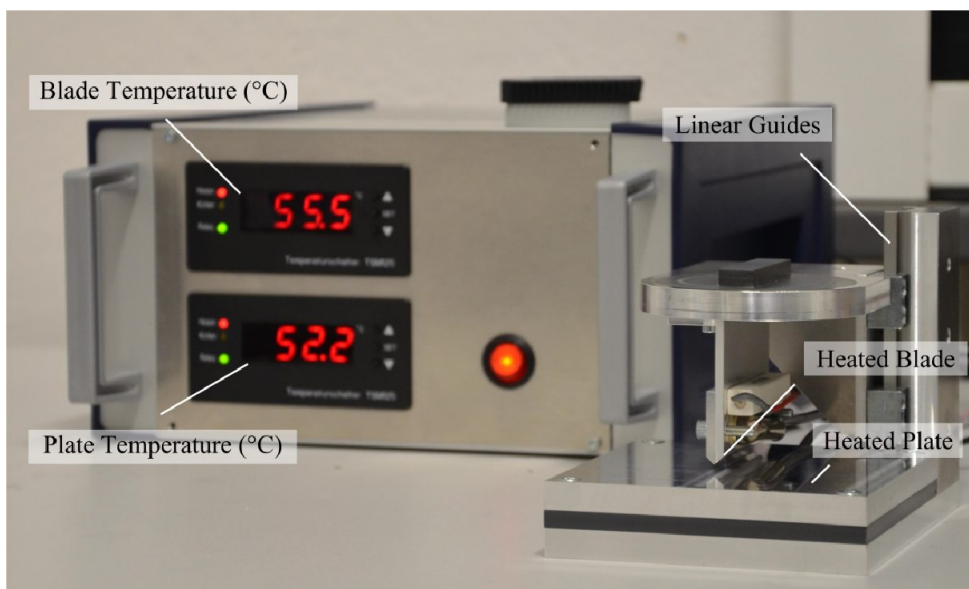


Figure 8: Photography of the self made POF cleaver.

## 5. CONCLUSIONS

For the realization of micro ring resonators within polymer foil extensive investigations have been carried out to determine optimal design parameters using simulation tools. Different loss mechanisms have been studied and surface roughness and bend losses have been identified to be the dominant ones.

Based on the simulations first ring resonators have been produced using microscope projection lithography.

## REFERENCES

- [1] Orghici, R., Lützow, P., Burgmeier, J., Koch, J., Heidrich, H., Schade, W., Welschoff, N., Waldvogel, S. R., "A microring resonator sensor for sensitive detection of 1,3,5- trinitrotoluene (TNT)," *Sensors* 10, 6788-6795 (2010)
- [2] Ovsianikov, A. Viertl, J., Chichkov, B., Oubaha, M., MacCraith, B., Sakellari, I., Giakoumaki, A., Gray, D., Vamvakaki, M., Farsari, M., Fotakis, C., "Ultra-Low Shrinkage Hybrid Photosensitive Material for Two-Photon Polymerization Microfabrication," *ACS Nano* 2, 2257-2262 (2008)
- [3] Gillrot, F., Vivien, L., Laval, S., Pascal, D., Cassan, E., "Size influence on the propagation loss induced by sidewalls roughness in ultrasmall SOI waveguides," *IEEE Photonics Technology Letter* 16, 1661-1663 (2004)
- [4] Xiao, Y., Pichler, E., Hofmann, M., Bethmann, K., Köhring, M., Willer, U., Zappe, H., "Towards integrated resonant and interferometric sensors in polymer films," *Procedia Technology* 15, 692-702 (2014)
- [5] Love, J. C., Wolfe, D. B., Jacobs, H. O., Whitesides, G. M., "Microscope Projection Photolithography for Rapid Prototyping of Masters with Micron-Scale Features for Use in Soft Lithography," *Langmuir* 17, 6005 – 6012 (2001).
- [6] Stefani, A., Nielsen, K., Rasmussen, H. K., Bang, O. "Cleaving of TOPAS and PMMA microstructured polymer optical fibers: Core-shift and statistical quality optimization," *Optics Communications* 285, 1825 – 1833 (2012)
- [7] Abdi, O., Wong, K. C., Hassan, T., Peters, K. J., Kowalsky, M. J., "Cleaving of solid single mode polymer optical fiber for strain sensor applications," *Optics Communications* 282, 856 – 861 (2009)